J. Fluid Mech. (1971), *vol.* 48, *part* 4, *pp.* 689–702
Printed in Great Britain

On the interpretation of some longitudinal dispersion experiments

By P. C. CHATWIN

Department of Applied Mathematics, The University of Liverpool

(Received 20 November 1970)

Experiments to determine the value of Taylor's longitudinal diffusivity in turbulent flows in open channels and circular pipes have produced results which are in many cases inconsistent with one another and with theoretical estimates due respectively to Elder (1959) and Taylor (1954). Neither is there general agreement on when Taylor's theory becomes applicable. In an attempt to clarify the discrepancies two well-known sets of experiments by Fischer (1966) and Taylor (1954) are re-examined by using a natural procedure which, it is argued, has certain advantages over more usual methods. It is shown that Fischer's observations in an open channel were not made at a sufficient distance downstream from the point of injection for Taylor's theory to apply but that they are consistent with a description of the early stages of the dispersion process due to Sullivan (1968). It is subsequently argued that these observations suggest that Elder's estimate of the diffusivity is too low for two reasons. The first is the error caused by assuming the existence of an eddy diffusivity calculated by means of Reynolds analogy and the second is the neglect of the viscous sublayer. On the other hand it is shown that some of Taylor's observations in a circular pipe are consistent with his theory, although the values of the diffusivity which best fit the data are about 25 % higher than Taylor's estimate, and it is suggested that this is for the same reasons as in the open channel. The paper concludes with a discussion of the effect of the viscous sublayer on the value of the longitudinal diffusivity. Partly on the basis of an approximate model it is argued that theoretical calculations which ignore the viscous sublayer are too low by amounts which depend on the Reynolds and Schmidt numbers and can be of the order of 20 %.

1. Introduction

This paper deals with the longitudinal dispersion of a passive contaminant in turbulent flow through circular pipes, and open channels of uniform rectangular cross-section. Throughout, U_0 denotes the discharge velocity, x measures distance in the longitudinal direction from a fixed cross-section, y and z are co-ordinates in the plane of the cross-section and t measures time. The distribution of concentration is denoted by $C(x, y, z, t)$ and its mean over a cross-section by $C_m(x, t)$.

For sufficiently large t, Taylor (1954) showed that

$$C \approx C_m \propto (t-t^*)^{-\frac{1}{2}} \exp\left\{-\frac{[(x-x^*)-U_0(t-t^*)]^2}{4K_0(t-t^*)}\right\}, \tag{1.1}$$

where x^*, t^* and K_0 are constants. K_0 will be referred to as the longitudinal diffusivity since (1.1) is consistent with the hypothesis that C_m is being diffused longitudinally across every cross-section at a rate $-K_0 \partial C_m/\partial x$ per unit area.

The values of x^* and t^* depend on the choices of the station $x = 0$ and the time $t = 0$. With the natural choices of $x = 0$ as the initial position of the centre of gravity of the cloud and $t = 0$ as the time of injection, it can be shown (Chatwin 1970) that the value of x^* depends on the initial distribution of concentration in such a way that $x^* = 0$ if this is uniform over every cross-section. With the same choice of $x = 0$ and $t = 0$ there are two contributions to the value of t^*. One depends on the initial distribution, and the second, normally by far the greater, is independent of the initial distribution and depends only on the variation of flow properties over the cross-section. A formula for this contribution to t^* is given in Chatwin (1970). However, the values of x^* and t^* are difficult to estimate accurately for any particular experiment, and, as will be argued in § 3, it is usually sufficient in the analysis of experiments to approximate (1.1) by

$$C \approx C_m \propto t^{-\frac{1}{2}} \exp\left\{-\frac{(x-U_0 t)^2}{4K_0 t}\right\}. \tag{1.2}$$

This is a good approximation for large values of t/t^* except very near the peak of C_m.

Calculations of the value of K_0 have been presented for a circular pipe of radius a (Taylor 1954) with the result

$$K_0 \approx 10{\cdot}1 a u_*, \tag{1.3}$$

and for an open channel of depth h (Elder 1959) with the result

$$K_0 \approx 5{\cdot}9 h u_*, \tag{1.4}$$

where u_* is the friction velocity. In both calculations the existence of an eddy diffusivity calculated by means of Reynolds analogy was assumed and the viscous sublayers were ignored. In addition Elder ignored the variation of the turbulence properties across the width of the channel although it is now known that this is unjustified in many natural channels, in which the value of K_0 may consequently be much higher than that given in (1.4) (Fischer 1966).

Experiments on longitudinal dispersion have normally been designed to answer one or more of the following questions.

(i) Is it true, as in (1.1) and (1.2), that C_m is a Gaussian function of x for sufficiently large t?

(ii) If so, how large is 'sufficiently large t'?

(iii) What is the appropriate value of K_0?

The answer to (i) is generally accepted to be in the affirmative and it is the answers to (ii) and (iii) which have lately aroused most interest and controversy (see Fischer 1966, p. 15). In an attempt to elucidate the controversy, some experiments by Taylor (1954) with a circular pipe and by Fischer (1966) with an open channel are re-examined in this paper and the conclusions arrived at differ somewhat from those originally put forward. An attempt to explain some of the differences is made which stresses the role of the viscous sublayer.

Both Taylor and Fischer made use of an approximation, which will be called the 'frozen-cloud approximation' in this paper, and it was felt necessary to discuss the errors introduced by this before examining the experimental results. This is the subject of § 2.

2. The frozen-cloud approximation and why it is unnecessary

A common technique in longitudinal dispersion experiments in turbulent flows is to place one or more probes at a *fixed* cross-section (say at $x = x_0$) and to measure the response as a function of t as the cloud of contaminant passes the probe. By suitable calibration this technique gives a direct record of $C_m(x_0, t)$. If x_0 is sufficiently large the bulk of the cloud of contaminant will pass the probe at values of t so that (1.2) holds approximately. Hence†

$$C_m(x_0, t) = At^{-\frac{1}{2}} \exp\left\{-\frac{(x_0 - U_0 t)^2}{4K_0 t}\right\}, \tag{2.1}$$

where A is a constant proportional to the total quantity of contaminant.

Now (2.1) shows that the graph of $C_m(x_0, t)$ against t is not symmetrical about $t = x_0/U_0$, because of the factors t^{-1} (in the argument of the exponential) and $t^{-\frac{1}{2}}$ (multiplying the exponential). This asymmetry is one manifestation of the fact that the portions of the cloud of contaminant which pass the probe first are 'younger' than those which pass later. Nevertheless, it has often been argued that this asymmetry may be small if the speed U_0 at which the cloud is being swept past the probe is much greater than the speed at which the cloud is evolving. The evolution is completely described as a diffusion process with diffusivity K_0. Thus at time t, the speed of evolution is, on dimensional grounds, a multiple of $(K_0/t)^{\frac{1}{2}}$. Thus at time $t = x_0/U_0$ a characteristic speed of evolution is $(K_0 U_0/x_0)^{\frac{1}{2}}$, and hence, if $U_0 \gg (K_0 U_0/x_0)^{\frac{1}{2}}$, that is if

$$(K_0/U_0 x_0)^{\frac{1}{2}} \ll 1, \tag{2.2}$$

the graph of $C_m(x_0, t)$, given by (2.1), against t might be nearly symmetrical. If so, then instead of (2.1),

$$C_m(x_0, t) \approx A(x_0/U_0)^{-\frac{1}{2}} \exp\left\{-\frac{(x_0 - U_0 t)^2}{4K_0 x_0/U_0}\right\}, \tag{2.3}$$

or equivalently, using (1.1),

$$C_m(x_0, t) \approx C_m(x', x_0/U_0), \tag{2.4}$$

where $x' - x_0 = x_0 - U_0 t$. It is the approximation (2.3) or (2.4) that will be called the 'frozen-cloud approximation'. It is due to Taylor (1954). Its advantage is that it is easier to analyze a Gaussian curve like (2.3) than a relatively complicated one like (2.1).

Nevertheless, since the arguments in the exponentials of (2.1) and (2.3) are different, the error involved in the approximation will always be substantial sufficiently far from the value $t = x_0/U_0$. The relative error is

$$\frac{C_m(x_0, t) - C_m(x', x_0/U_0)}{C_m(x_0, t)}.$$

† The argument of this section remains valid (with obvious changes in notation) if it is based on (1.1), rather than (1.2).

Using (2.1) and (2.3) it is found that

$$\frac{C_m(x_0,t)-C_m(x',x_0/U_0)}{C_m(x_0,t)} = 1-(1-\epsilon X)^{\frac{1}{2}}\exp\left\{\frac{\epsilon X^3}{2(1-\epsilon X)}\right\}, \tag{2.5}$$

where

$$X = \frac{(x_0-U_0t)}{(2K_0x_0/U_0)^{\frac{1}{2}}}, \quad \epsilon = \left(\frac{2K_0}{U_0x_0}\right)^{\frac{1}{2}}. \tag{2.6}$$

As is well-known $(2K_0x_0/U_0)^{\frac{1}{2}}$ is the standard deviation, σ, of the Gaussian curve (1.2) at time x_0/U_0. Hence X is $(x'-x_0)/\sigma$ and is the variable that would be used were the functions $C_m(x_0,t)$ and $C_m(x',x_0/U_0)$ expressed in standard measure. Furthermore, ϵ is equal to σ/x_0, showing that (2.2) (which is equivalent to $\epsilon \ll 1$) implies that the standard deviation of the cloud is much smaller than the distance it has travelled. If $\epsilon \ll 1$ and if $|\epsilon X^3|$ is also small the relative error given by (2.5) is approximately

$$\tfrac{1}{2}\epsilon(X-X^3)$$

and is therefore small. However, for values of X of $O(\epsilon^{-\frac{1}{3}})$ or greater the exponential in (2.5) becomes substantially different from one. Therefore the argument leading to (2.2) breaks down essentially because it ignores those parts of the cloud that are observed at values of t substantially different from x_0/U_0. Figure 1 plots the relative error given by (2.5) for three values of ϵ, and these graphs confirm the points above.

Thus any deduction from experiments in which the frozen-cloud approximation is invoked must be examined carefully if the values of $C_m(x_0,t)$ in the tails of the

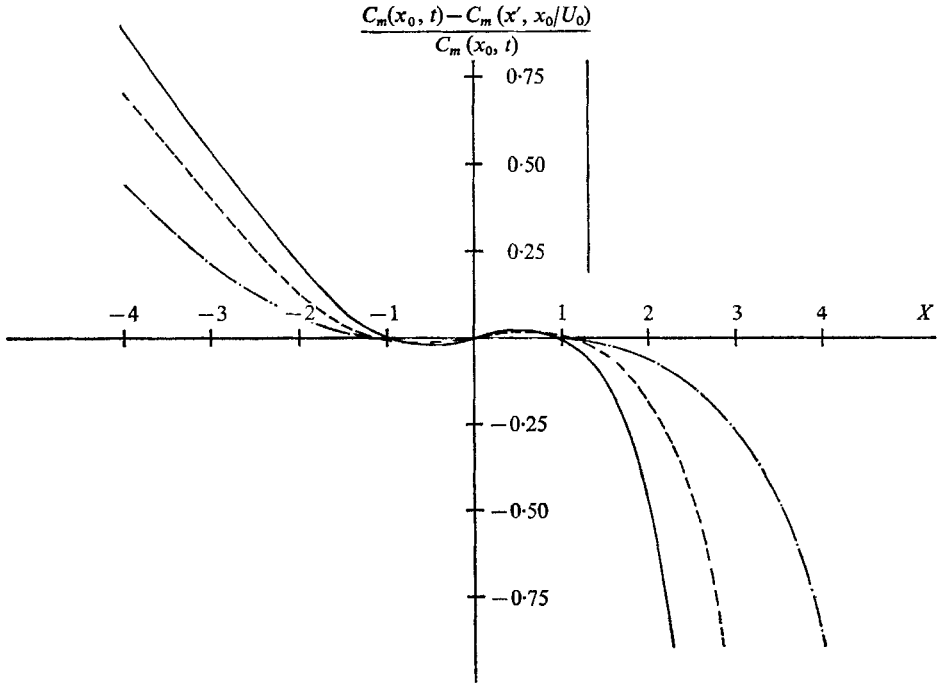

FIGURE 1. The relative error caused by use of the frozen-cloud approximation for three values of $\epsilon = (2K_0/U_0x_0)^{\frac{1}{2}}$. ——, $\epsilon = 0{\cdot}10$; - - - - -, $\epsilon = 0{\cdot}05$; —·—·—·, $\epsilon = 0{\cdot}02$.

distribution are important. This is true in calculations of the integral moments of the distribution, although it is known (Fischer 1966) that the use of the frozen-cloud approximation in relating the second moments of the observed and approximate distributions is valid if ϵ is small. But higher moments than the second are not so simply related so that, for example, the scheme outlined by Chatwin (1970) in which non-Gaussian curves observed for fixed time are described in terms of their integral moments needs re-examination if it is to apply to non-Gaussian curves observed at a fixed probe.

The preceding discussion emphasizes the care with which the frozen-cloud approximation should be used. It will now be shown that its use is not normally necessary, since there is a natural way of analyzing the values of $C_m(x_0, t)$ in order to answer the questions (i), (ii) and (iii) of § 1 which does not use the frozen-cloud approximation.

For, if (2.1) holds,

$$[t \log_e \{A/C_m t^{\frac{1}{2}}\}]^{\frac{1}{2}} = \left[\frac{x_0}{2K_0^{\frac{1}{2}}} - \frac{U_0 t}{2K_0^{\frac{1}{2}}}\right]. \tag{2.7}$$

The value of A can be estimated from the values of $C_m(x_0, t)$ near and at the peak. The left-hand side of (2.7) can then be calculated and plotted against t. If the graph is a straight line question (i) is answered affirmatively and one has an upper limit on the minimum value of t for which (1.2) holds. Furthermore the values of U_0 and K_0 can be estimated from the slope and intercept of the straight line, assuming x_0, the distance of the probe downstream from the point of injection, is known. On the other hand if the graph is not a straight line nothing can be said about questions (i) and (iii) but one has a lower limit on the value of t for which (1.2) holds.

Applications of the procedure just outlined will be given in the next two sections but one or two general comments seem appropriate here. First the general shape of the graph of $[t \log_e \{A/C_m t^{\frac{1}{2}}\}]^{\frac{1}{2}}$ against t is not very sensitive to the value of A. Only those points near $t = x_0/U_0$ are visibly affected by a change in A of a few percent and the requirement that the graph passes smoothly through such points enables A to be determined to within 1 or 2 %. The second point is that the value of C_m is extremely sensitive to the value of U_0 and also, but to a lesser extent, to that of K_0. In fact errors ΔA, ΔK_0 and ΔU_0 in the values of A, K and U_0 cause an error ΔC_m in the value of C_m determined by (2.1), which satisfies to first order

$$\frac{\Delta C_m}{C_m} = \frac{\Delta A}{A} + \frac{X^2}{2(1-\epsilon X)} \frac{\Delta K_0}{K_0} + \frac{X}{\epsilon} \frac{\Delta U_0}{U_0},$$

where X and ϵ are defined in (2.6). For a typical value of ϵ of 0·04 a 1 % error in U_0 causes a 25 % error in C_m at $X = 1$ and a 100 % error in C_m at $X = 4$. For the same value of ϵ a 1 % error in K_0 causes about a 0·5 % error in C_m at $X = 1$ but about a 9 % error at $X = 4$. The present procedure has the important advantage that the values of U_0 and K_0 can be estimated to provide the best fit to all the data in contrast to some other methods which only use the value of C_m at one or two points.

3. Analysis of experiments by Fischer

Fischer (1966) conducted a large number of careful and detailed experiments in open channels of various cross-sections. Among these were several in a laboratory flume of rectangular cross-section, 110 cm wide, in which the flow properties varied little across the width of the channel. Fischer therefore argued that the experimental conditions were those under which Elder's calculation leading to the result (1.4) were made.

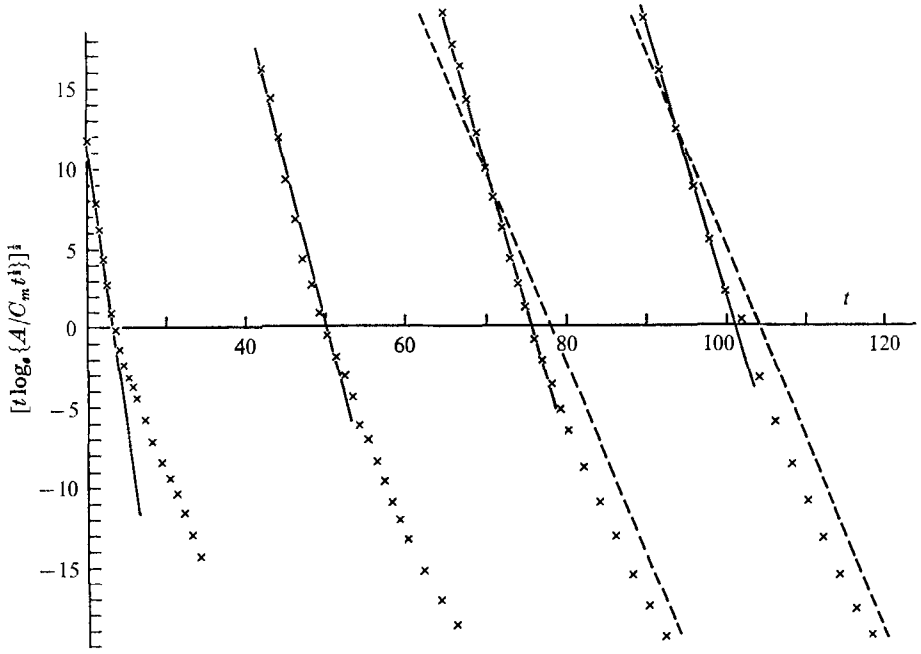

FIGURE 2. The data from series 2600 of Fischer (1966) plotted according to the procedure discussed in the text. The observations were made at four stations at 706, 1406, 2106 and 2806 cm downstream from the point of injection. The broken lines are determined by $U_0 = 26{\cdot}9$ cm/sec and $K_0 = 117$ cm^2/sec – the values given by Fischer. The full lines fit the front portion of each curve with values of U and K given in table 1.

In series 2600 of his experiments the values of h, U_0 and u_* were estimated as 6·9 cm, 26·9 cm/sec and 1·36 cm/sec respectively and $C_m(x_0, t)$ was determined at four values of x_0, viz. = 706 cm, 1406 cm, 2106 cm, and 2806 cm. The results of applying the procedure based on (1.2) and described above to the four sets of data are shown in figure 2.

The most striking fact is that none of the curves is a straight line so that the data cannot be fitted by curves of the form (2.1). It is therefore concluded that insufficient time has elapsed (or equivalently that the probes are at an insufficient distance downstream) for (2.1) to be a correct description. (The same conclusions are true for series 2700 of Fischer's experiments although the curves are not given here.) This is in contrast to Fischer's interpretation of the same data. He argued that the final two experiments are consistent with (2.1) with a value of

K_0 of 117 cm²/sec† (and U_0 as 26·9 cm/sec). The straight lines that would be given were this true are shown as dashed lines in figure 2.

All four curves in figure 2 differ from straight lines in that they curve towards the axis for t greater than x_0/U_0 indicating that they decay more slowly than if they were Gaussian. Details of the variation of $C(x, y, z, t)$ over the depth are given in Fischer (1966). These show, first, that at large values of t the contaminant is concentrated near the bottom of the channel and, secondly, that it is in this region that the differences between $C(x, y, z, t)$ and the values predicted by the analysis leading to (1.4) are most marked. Both these points suggest that the reason that the asymptotic state has not been reached is connected with the mechanics of the dispersion process in the region near the bottom of the channel, perhaps in the viscous sublayer.

For times less than x_0/U_0 which is very nearly the time at which $C_m(x_0, t)$ attains its peak, each of the four curves in figure 2 is straight. Therefore the forward portion of the graph of each $C_m(x_0, t)$ (but *only* the forward portion) can be described by a curve of the form (2.1), viz.

$$C_m(x_0, t) = At^{-\frac{1}{2}} \exp\left\{-\frac{(x_0 - Ut)^2}{4Kt}\right\}, \tag{3.1}$$

where, as table 1 shows, the values of U and K differ for each curve and are therefore not in general equal to U_0 and K_0 respectively. It is possible to interpret these observations in terms of a description of the early stages of the dispersion process in open channels due to Sullivan (1968).

x_0 (cm)	706	1406	2106	2806
A	511·3	671·2	921·5	995·2
U (cm/sec)	30·4	28·2	27·9	27·8
K (cm²/sec)	16·9	46·9	60·7	63·0

TABLE 1. Values of A used in plotting the data of figure 2 together with the values of U and K for the full lines which fit the front portions of each curve

Sullivan showed that prior to the period in which the whole graph of $C_m(x, t)$ is Gaussian there are two preliminary stages in which only the forward portion of the curve is Gaussian.

The first of these stages exists for t such that

$$1 \lesssim tu_*/h \lesssim 4. \tag{3.2}$$

During this period the forward portion of the graph of $C_m(x, t)$ is almost wholly due to contaminant in the upper half of the channel, and provided $tu_*/h \gtrsim 1$ the material in this region has sampled all the region because of the relatively high intensity of vertical mixing there. On the other hand, experiments showed that provided $tu_*/h \lesssim 4$ relatively little of the material in the upper half of the flow which contributes to the forward portion of $C_m(x, t)$ has dispersed into the

† This estimate was based on equating the measured value of the second moment to $2K_0x_0/U_0^3$, the theoretical value given by (2.1), but this equation is incorrect since (2.1) is not applicable as the argument in the text shows.

slower-moving lower half of the flow – a region of relatively low intensity of vertical mixing. These arguments suggest and experiments confirm that, if (3.2) holds, the forward portion of the graph of $C_m(x,t)$ is Gaussian with values of U and K determined solely by conditions in the upper half of the channel. Sullivan's experiments showed that in this first stage

$$U \approx 1{\cdot}10U_0, \quad K \approx 0{\cdot}0053u_* h\left\{\left(\frac{U_0}{u_*}\right)^2 - 295\right\}. \tag{3.3}$$

The same first stage should be observable in the curve of $C_m(x_0,t)$ provided

$$1 \lesssim x_0 u_*/hU_0 \lesssim 4.$$

The first curve in figure 2 is such that $x_0u_*/hU_0 \approx 4{\cdot}5$, suggesting that the first stage has just finished. This is confirmed by the measured values of U and K given in table 1. The measured value of U, 30·4 cm/sec, is 1·13 times Fischer's estimate of U_0, 26·9 cm/sec. On the other hand the evidence of the later entries in table 1 is that U_0 is nearer 27·8 cm/sec and $30{\cdot}4/27{\cdot}8 = 1{\cdot}09$ which is just less than the value 1·10 given in (3.3). The value of K given by (3.3) is 6·11 cm^2/sec in contrast to the measured value of 16·85 cm/sec, which suggests that the transition from the first stage to a second stage is in progress.

This second stage exists when the contaminant has had time to sample all the cross-section excluding the viscous sublayer and estimates suggest that this occurs for t such that

$$tu_*/h \gtrsim 10. \tag{3.4}$$

When this is satisfied the forward portion of the graph of $C_m(x,t)$ is almost wholly due to material not in the viscous sublayer, so that as in the first stage the forward portion is described by a Gaussian curve with values of U and K now determined by conditions in that part of the channel above the viscous sublayer. The value of U is equal to the average of the longitudinal velocity in this region, and this varies from U_0 to $1{\cdot}02U_0$ depending on the height of the viscous sublayer; the value of K should equal Elder's value (1.4) if Reynolds analogy holds.

The values of x_0u_*/hU_0 for the last two curves of figure 2 are 15·4 and 20·5 respectively so that the second stage description should apply. In fact the observed values of U are both close to 27·8 cm/sec (suggesting that U_0 lies between 27·3 and 27·8 cm/sec) and the values of K are $6{\cdot}5hu_*$ and $6{\cdot}7hu_*$ respectively suggesting that Elder's estimate (1·4) should be amended to about $6{\cdot}6hu_*$. If this is so the error in Elder's estimate can be attributed to the inadequacy of Reynolds analogy.

In the second stage the whole curve is not Gaussian because of the material in the slow-moving viscous sublayer which causes the curve of $C_m(x,t)$ to have a long tail, and so that of $C_m(x_0,t)$ to decay more slowly than if it were derived from a Gaussian curve. This is consistent with Fischer's observations. During the whole of the second stage material is gradually diffusing across the boundary of the viscous sublayer where the intensity of lateral mixing is very low. Eventually, but it is difficult to quantify this word in view of the ignorance of the mechanics of the motion in the viscous sublayer, the whole curve will be described by (2.1).

The final value of K will be greater than that in the second stage and an estimate of its value will be given in § 5. What is certain is that any such estimate must involve consideration of the viscous sublayer.

The conclusions of this section are not changed if Fischer's experiments are analyzed using (1.1) rather than (1.2), but it is worth describing how this is done since there are one or two points of interest. Equation (2.7) derived from (1.2) must now be replaced by the analogous expression derived from (1.1), viz.

$$[(t-t^*)\log_e\{A/C_m(t-t^*)^{\frac{1}{2}}\}]^{\frac{1}{2}} = \left[\frac{(x_0-x^*)}{2K_0^{\frac{1}{2}}} - \frac{U_0(t-t^*)}{2K_0^{\frac{1}{2}}}\right], \tag{3.5}$$

and in order to plot the left-hand side against $(t-t^*)$, as the procedure described in § 2 directs, an estimate of t^* (but not x^*) is necessary. This can be obtained from the expression given by Chatwin (1970).

For the first curve in figure 2 the value of t^*, which here depends only on the flow properties in the upper half of the cross-section, is estimated to be 0·04 sec and the plot of the left-hand side of (3.5) against $(t-t^*)$ is negligibly different from the first curve in figure 2.

On the other hand the value of t^* for the last two curves in figure 2 is determined by the flow properties in the whole cross-section excluding the viscous sublayer. A rough estimate of its value is 6 sec, based on using the logarithmic velocity profile and Reynolds analogy over the whole cross-section (leading to errors which are difficult to estimate and therefore difficult to reduce). With this value of t^*, the new third and fourth curves in figure 2 are, except for a displacement of 6 sec, almost indistinguishable from the original ones. In particular the forward portions of the curves are straight, with the same slopes as the originals.

From any *one* of these two curves it is not possible to determine the values of U and K (which are not necessarily equal to U_0 and K_0–see the remark after (3.1)) since the values of x^* and t^* are unknown. However, since the shape of the curves is insensitive to the value of t^*, the values of t where the curves intercept the time axis can be found from figure 2. In fact $t = 75{\cdot}8$ sec for the third curve and $t = 101{\cdot}2$ sec for the fourth curve. Therefore, using the known values of x_0 in (3.5), it follows that

$$\left.\begin{aligned} 2106 - 75{\cdot}8U &= x^* - Ut^*, \\ 2806 - 101{\cdot}2U &= x^* - Ut^*. \end{aligned}\right\} \tag{3.6}$$

Thus $U = 27{\cdot}56$ cm/sec which is close to the value determined earlier in this section. It may therefore be concluded that analysis on the basis of (1.2), rather than (1.1), does not alter the estimated value of U (and hence of K) in experiments like Fischer's.

A value of $(x^* - Ut^*)$ can be deduced from (3.6), but is not very reliable since it is the difference of two large quantities. In order to determine x^* and t^*, data must be taken at several values of x_0.

4. Analysis of Taylor's experiments

Taylor (1954) performed several experiments in a circular pipe with $a = 0{\cdot}476$ cm. Figures 3 and 4 show the results of applying the procedure based on (1.2) and described in § 2 to the data shown in figures 7 and 8 of Taylor's paper. The values of C_m were read directly from Taylor's graphs and it was assumed that C_m was zero at the extreme points recorded.

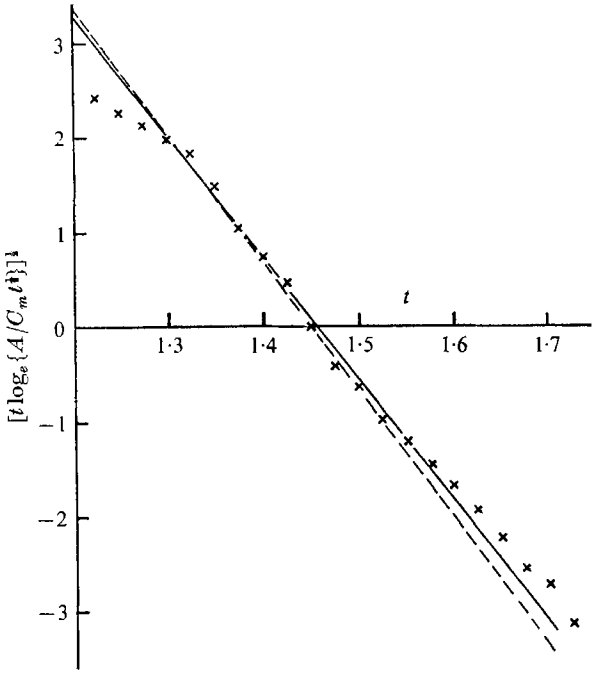

FIGURE 3. The data from figure 7 of Taylor (1954) plotted according to the procedure discussed in the text. The values of u_*, x_0 and a are 12·65 cm/sec, 322 cm and 0·476 cm. The full line is that given by $U_0 = 221$ cm/sec and $K_0 = 75$ cm²/sec. The broken line is that given by Taylor's values, $U_0 = 222$ cm/sec and $K_0 = 70$ cm²/sec.

Two points of difference from the curves in figure 2 are evident. First the points are more scattered and second there is no general tendency for the curves in figures 3 and 4 to veer away from straight lines for $t > x_0/U_0$ as there was in figure 2. Indeed it seems reasonable to argue that both curves are straight within experimental error and the full lines in figures 3 and 4 are those which seem the best fit. The dashed lines in figures 3 and 4 are those corresponding to the values of U_0 and K_0 given by Taylor.†

The fact that these curves can be fitted by straight lines is evidence that x_0 is sufficiently large for the final asymptotic stage to have been reached. The values of $x_0 u_*/aU_0$ for the data of figures 3 and 4 are 38·7 and 212·8 respectively. These

† Taylor estimated K_0 by measuring the two values of t at which C_m attained one half of its peak value and then equating their difference to $\{4K_0 x_0 \log_e 2/U_0^3\}^{\frac{1}{2}}$, which is the result given by assuming the validity of the frozen-cloud approximation and using (2.3).

are much greater than 20·5, the maximum value of the corresponding parameter $x_0 u_*/hU_0$ recorded in Fischer's experiments discussed in § 3, where it was shown that the value of $x_0 u_*/hU_0$ determined the stage of development of $C_m(x_0, t)$ towards its final state (2.1).

In the curve shown in figure 3, the value of K_0/au_* given by the full line is 12·5 while that given by Taylor's value is 11·6. The corresponding values for figure 4 are 13·7 and 12·8 respectively. The theoretical value (see (1.3)) is 10·1.

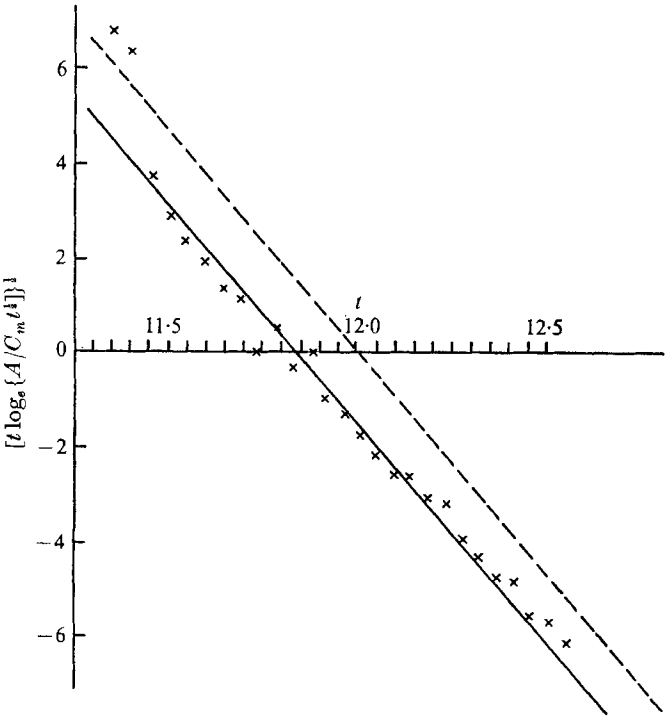

FIGURE 4. The data from figure 8 of Taylor (1954) plotted according to the procedure discussed in the text. The values of u_*, x_0 and a are 8·45 cm/sec, 1631 cm and 0·476 cm. The full line is that given by $U_0 = 137{\cdot}8$ cm/sec and $K_0 = 55$ cm^2/sec. The broken line is that given by Taylor's values, $U_0 = 136$ cm/sec and $K_0 = 51{\cdot}3$ cm^2/sec.

5. The effect of the viscous sublayer on K_0

The interpretations presented in the last two sections suggest that K_0 is greater than the estimates (1.3) and (1.4). It was shown in § 3 that the evidence of Fischer's experiments is that, in an open channel, at least some of this discrepancy is due to the ignoring of the viscous sublayer in the derivation of (1.4) and there is no reason why the same should not be true in a circular pipe. Some arguments are now presented to support this view.

It is well-known (Taylor 1954, Batchelor 1966) that the longitudinal velocity of a marked fluid particle in an open channel of uniform cross-section or in a circular pipe, is a stationary random function of t with mean U_0. Hence, by stationarity

$$\overline{(u(t)-U_0)\,(u(t+\xi)-U_0)} = u_*^2 R(\xi),$$

where the overbar denotes an ensemble mean. The value of K_0 can be written in terms of $R(\xi)$ in the following way:

$$K_0 = u_*^2 \int_0^\infty R(\xi)\, d\xi. \tag{5.1}$$

Now

$$\int_0^\infty R(\xi)\, d\xi$$

is a measure of the time taken for a fluid particle to sample the whole cross-section. The time taken to sample the part of the cross-section outside the viscous sublayer is, on dimensional grounds, of order a/u_* in a circular pipe and h/u_* in an open channel, and these times give values of K_0 consistent with (1.3) and (1.4). But these times are not normally accurate estimates of the times taken to sample the whole cross-section since within the viscous sublayer the properties of the turbulence depend directly on the viscosity ν, and the lateral mixing sufficiently near the wall is dominated by molecular processes whose intensity is measured by the molecular diffusivity κ. This suggests that the time taken to sample the whole cross-section is greater than a/u_* or h/u_* by an amount that increases as κ decreases and as the height of the viscous sublayer increases (that is as the Reynolds number decreases).

An estimate of the increase can be made if it is assumed that the lateral transfer of contaminant everywhere including the sublayer obeys the gradient law of diffusion with a diffusivity which is the sum of the molecular diffusivity κ and an eddy diffusivity κ_T calculated by means of Reynolds analogy. This assumption is not theoretically well-founded; in particular the lateral transfer of contaminant within the sublayer depends on κ whereas the lateral transfer of momentum does not and this makes the validity of Reynolds analogy very unlikely. Nevertheless, similar assumptions have been made in heat transfer theory with reasonable agreement with experiments (Monin & Yaglom 1966, pp. 247–261). It seems worthwhile to pursue the same assumption here if only to produce a target to be shot down!

Consider an open channel of depth h. There are two contributions to the value of K_0. The first is the direct effect of longitudinal diffusion with an estimated value of $0{\cdot}07hu_*$ (Elder 1959) which is small and negligibly affected by the sublayer. The second is the effect of the interaction between lateral diffusion and longitudinal advection. If the gradient law of diffusion holds this can be written as an integral with respect to y where $y = 0$ is the wall and $y = h$ the free surface; viz.

$$\frac{1}{h}\int_0^h \frac{dy}{\kappa+\kappa_T}\left\{\int_0^y u(y')\, dy'\right\}^2,$$

where $u(y)$ is the difference between the mean longitudinal velocity at height y and the discharge velocity U_0 (Ellison 1960). Thus, combining the two contributions,

$$K_0 = 0{\cdot}07hu_* + \frac{1}{h}\int_0^h \frac{dy}{\kappa+\kappa_T}\left\{\int_0^y u(y')\, dy'\right\}^2. \tag{5.2}$$

In evaluating (5.2) Elder assumed that $\kappa_T(y)$ was a parabolic function of y and

$u(y)$ a logarithmic function of y throughout the channel, that is he ignored the change in these functions within the sublayer. However (5.2) can be written

$$K_0 = 0{\cdot}07hu_* + \frac{1}{h}\int_\delta^h \frac{dy}{\kappa+\kappa_T}\left\{\int_0^y u(y')\,dy'\right\}^2 + \frac{1}{h}\int_0^\delta \frac{dy}{\kappa+\kappa_T}\left\{\int_0^y u(y')\,dy'\right\}^2, \quad (5.3)$$

where δ is the height of the viscous sublayer. Since $\delta/h \ll 1$ and $\kappa/\kappa_T \ll 1$ if $y > \delta$ the sum of the first two terms is approximately the value of K observed in Sullivan's second stage. It was suggested in § 3 that this is near to $6{\cdot}6hu^*$ (rather than $5{\cdot}9hu_*$ as suggested by Elder's estimate (1.3)). Therefore

$$K_0 \approx 6{\cdot}6hu_* + \frac{1}{h}\int_0^\delta \frac{dy}{\kappa+\kappa_T}\left\{\int_0^y u(y')\,dy'\right\}^2. \quad (5.4)$$

The integral in (5.4) can be approximately evaluated by replacing u and κ_T by the first terms in their Maclaurin expansions provided δ is consistently defined. Now

$$u(y) = -U_0 + u_*\left\{\frac{u_* y}{\nu} + O\left(\frac{u_* y}{\nu}\right)^4\right\}, \quad (5.5)$$

and by Reynolds analogy, and data in Townsend (1956, pp. 220–1),

$$\kappa_T = -\frac{\overline{u'v'}}{du/dy} \approx 0{\cdot}0006\nu\left\{1 + O\left(\frac{u_* y}{\nu}\right)\right\}, \quad (5.6)$$

where u' and v' are the longitudinal and vertical components of the velocity fluctuation. On substituting in (5.4) and integrating it follows to first order that

$$K_0 \approx 6{\cdot}6hu_*\left\{1 + 83{\cdot}8\left(\frac{U_0}{u_*}\right)^2\left(\frac{\nu}{u_* h}\right)^2 \log_e\left[1 + 0{\cdot}0006\left(\frac{u_*\delta}{\nu}\right)^3\frac{\nu}{\kappa}\right]\right\}. \quad (5.7)$$

A calculation that is similar in all respects can be made for a circular pipe with the result

$$K_0 \approx 10{\cdot}1au_*\left\{1 + 27{\cdot}5\left(\frac{U_0}{u_*}\right)^2\left(\frac{\nu}{u_* a}\right)^2 \log_e\left[1 + 0{\cdot}0006\left(\frac{u_*\delta}{\nu}\right)^3\frac{\nu}{\kappa}\right]\right\}. \quad (5.8)$$

The height of the viscous sublayer must on dimensional grounds be proportional to ν/u_*. The constant of proportionality depends on the particular criterion used to define δ, but a value of 5 is commonly used. Thus take

$$\delta = 5\nu/u_*.$$

In Fischer's experiments (§ 3)

$$U_0/u_* = 20{\cdot}4, \quad \nu/u_* h = 1{\cdot}07 \times 10^{-3}.$$

The value of κ is not known but a typical value is $10^{-5}\,\mathrm{cm}^2/\mathrm{sec}$. With these values (5.7) gives

$$K_0 \approx 6{\cdot}6hu_*\{1 + 0{\cdot}17\} \quad (5.9)$$

so that, with this model, the true value of K_0 is 17 % greater than that observed in Sullivan's second stage, that is calculated with the sublayer neglected.

For Taylor's experiments the same values of δ and κ substituted in (5.8) lead to

$$K_0 \approx 10{\cdot}1au_*\{1+0{\cdot}12\},$$

for figure 3 and

$$K_0 \approx 10{\cdot}1au_*\{1+0{\cdot}23\},$$

for figure 4. These are about 10 % lower than the values given by the full lines of figures 3 and 4. Two possible causes of the discrepancy are the inadequacy of the model used in this section to describe diffusion in the viscous sublayer and an error in the estimate (1.3) caused by the use of Reynolds analogy, equivalent to that which was suggested to exist in the open channel estimate, (1.4), and which was discussed in § 3.

It is therefore concluded that neglect of the viscous sublayer may well cause errors of the order of 10–20 % in the calculated values of K_0, and that these values may themselves have errors of the order of 10 % if Reynolds analogy is assumed to hold in the bulk of the flow.

I am grateful to Professor G. K. Batchelor for several conversations on the material discussed in § 5, and to him and Professor H. B. Fischer for their comments on earlier drafts of this paper.

REFERENCES

BATCHELOR, G. K. 1966 *Proc. 2nd Australasian Conference on Hydraulics and Fluid Mechanics*, Auckland.

CHATWIN, P. C. 1970 *J. Fluid Mech.* **43**, 321.

ELDER, J. W. 1959 *J. Fluid Mech.* **5**, 544.

ELLISON, T. H. 1960 *J. Fluid Mech.* **8**, 33.

FISCHER, H. B. 1966 *California Institute of Technology, Rep.* KH-R-12.

MONIN, A. S. & YAGLOM, A. M. 1966 *Statistical Hydromechanics*. U.S. Dept. of Commerce, Washington D.C.

SULLIVAN, P. J. 1968 Ph.D. Thesis, University of Cambridge.

TAYLOR, G. I. 1954 *Proc. Roy. Soc.* A **223**, 446.

TOWNSEND, A. A. 1956 *The Structure of Turbulent Shear Flow*. Cambridge University Press.